New Folder Name Harmonic Demodulation

HARMONIC DEMODULATION OF NON - STATIONARY SHOT NOISE

Malcolm B Gray
Andrew J Stevenson
Hans-A Bachor
David E McClelland

Technical Report
2/92

The Australian National University

Department of Physics & Theoretical Physics
Faculty of Science
GPO BOX 4, Canberra ACT 2601 Australia
Telephone : 06 249 4105 / 2811 (Authors)
06 249 2747 (Departmental Sec.)
Fax : 06 249 0741 (International +61 62 49 0741)

Harmonic demodulation of non-stationary shot noise

Malcolm B Gray

Andrew J Stevenson

Hans -A Bachor

David E McClelland

Department of Physics and Theoretical Physics

Faculty of Science

The Australian National University

GPO Box 4 Canberra ACT 2601

Australia

Abstract

We report on experimental demodulation of non-stationary shot noise, associated with strongly modulated light. For sinusoidal modulation and demodulation, measurements confirm theoretical predictions of 1.8 dB excess noise in the signal quadrature and 3 dB noise reduction in the opposite quadrature, relative to the standard quantum limit. Demodulation with a third harmonic produces noise correlated with that due to the fundamental. Reduction of excess noise by 0.8 dB in the signal quadrature, by combining the fundamental and third harmonics in a 2:1 ratio, is shown to be feasible.

Optical modulation is commonly employed to enhance small signal sensitivity in interferometric sensors and homodyne detection systems[1,2]. In quantum noise limited systems, however, modulation may also lead to observable non-stationary shot noise. An unwanted side-effect in simple demodulation and synchronous detection schemes is excess noise in the signal quadrature.

Non-stationary shot noise has been implicated in the anomalously high noise floor observed in the Garching prototype gravitational wave detector[3], and has recently been demonstated experimentally by both Mio et al[4] and Meers et al[1]. In the latter experiment, sinusoidal modulation and demodulation caused the noise level to vary by about 2.5 dB (peak-peak) with demodulation phase. In our experiment, we observed 4.8 dB (peak-peak) phase dependence, close to the maximum predicted for fully sinusoidally modulated light, using a Michelson interferometer with high fringe contrast.

The excess noise in the signal quadrature may be cancelled by using more advanced modulation and demodulation schemes[1,3]. In this letter we demonstrate that the addition of a third harmonic in the demodulation waveform introduces correlated noise, allowing partial cancellation of the excess noise in the signal quadrature.

Quantum noise is associated with any optical intensity measurement, and appears as flat spectrum photocurrent fluctations with variance proportional to photocurrent i(t)[5]. Non-stationary quantum noise $i_n(t)$ in the photocurrent i(t) is characterised by a time-dependent autocorrelation[3]:

$$\langle i_n(t)\, i_n(t+\tau)\rangle = e\, i(t)\, \delta(\tau) \qquad (1)$$

where e is the electronic charge and $\delta(\tau)$ is the Dirac delta function.

Optical modulations shift the signal spectrum to higher frequencies. Baseband signals are generally recovered by feeding the photocurrent (signal + noise) into a mixer where it is multiplied by a periodic demodulating function D(t). The autocorrelation of the quantum noise $y_n(t)$ at the mixer output is

$$\langle y_n(t)\ y_n(t+\tau)\rangle \quad = \quad e\ D^2(t)\ i(t)\ \delta(\tau) \qquad (2)$$

The instantaneous power spectral density can be determined from the Fourier transform of (2).

Experimentally, signals are extracted by tuning a receiver, with a finite integration time T, to the desired signal frequency f. To resolve spectral information, T must be much greater than the demodulation period. The quantum noise power spectral density (assuming a single sided power spectrum) is then

$$P_n(f,t) \quad = \quad 2\,e\,\overline{D^2(t)\ i(t)} \qquad (3)$$

where the bar denotes an average performed over the integration time T of the receiver. This spectrum is flat (independent of frequency f) but the average on the RHS may vary slowly compared to T.

Of particular interest is an interferometer, with high fringe visibility, set to a dark fringe, and subject to deliberate internal phase modulation. In the

absence of other signals, sinusoidal phase modulation at a frequency f_m produces a photocurrent

$$i(t) = i_0 [1 - \cos(4\pi f_m t)] \quad (4)$$

where i_0 is the mean photocurrent. Demodulation with any periodic waveform with a fundamental frequency f_m will recover the baseband signal spectrum. The simplest demodulation waveform is :

$$D(t) = \sqrt{2} \sin [2\pi f_m t + \varphi(t)] \quad (5)$$

where $\varphi(t)$ is the offset phase (constant for synchronous demodulation). The noise power spectrum is obtained by substituting Eqs. (4) and (5) into Eq. (3):

$$P_n(f,t) = P_{sql} [1 + {}^1/_2 \cos [2\varphi(t)]] \quad (6)$$

where $P_{sql} = (2 e i_0 / T)$ is the noise power at the standard quantum limit for a constant photocurrent i_0. The phase dependence is caused by intensity modulation resulting from the deliberate optical phase modulation. (Typical signals have negligible effect on shot noise.) Maximum signal demodulation requires $\varphi = 0$, which corresponds, unfortunately, to an increased noise power of $3P_{sql}/2$. Likewise, setting the demodulation phase in quadrature with the signal ($\varphi = \pi/2$) results in a reduced noise floor of $P_{sql}/2$.

The reason for the phase dependence in Eq. (6) can be seen in a heuristic picture of the time domain process of demodulation (see Fig. 1): A modulated noise function is multiplied by in-phase ($\varphi = 0$) and quadrature ($\varphi = \pi/2$) waveforms. The in-phase waveform "picks out" non-stationary noise

better than the quadrature waveform. Eqs. (3) - (5) imply that any modulated photocurrent exhibits phase-dependent shot noise when demodulated at half of the intensity modulation frequency.

The arrangement shown in Fig. 2 was implemented to demonstrate the phase dependence in Eq. (6). A Michelson interferometer was locked midway between dark and bright fringes, and a resonant phase modulator in one arm produced almost complete intensity modulation at 75MHz. The interferometer was locked by minimising the second harmonic (150 MHz) in the intensity spectrum, via a piezo mounted mirror in one arm. The maximum detected optical power at 1064nm was around 5mW, with a minimum of 0.17mW, a fringe visibility of 0.935.

To observe phase dependent noise, a demodulation frequency of 37.5 MHz was required. Offsetting the frequency slightly from 37.5 MHz produces a slow monotonic variation in the phase in Eq. (6), effectively scanning $\varphi(t)$ through all values between 0 and 2π repeatedly. The RMS noise will oscillate between the two extremes allowed by Eq. (6) at a rate equal to twice the demodulation frequency offset.

In Fig. 3(a), the demodulated shot noise is plotted against time, for a demodulation frequency offset of a few Hz. The observed peak-peak variation is very close to the 4.8 dB predicted for completely sinusoidally modulated light. The effect of sweeping the demodulation frequency offset through zero is shown in Fig. 3(b). The receiver post-detection bandwidth has been deliberately reduced to average out oscillations above 100 Hz. When the demodulation frequency is sufficiently far from 37.5 MHz, the observed noise

averages to the standard shot noise level, highlighting the 1.8 dB noise penalty in the signal quadrature.

This excess noise can be partially cancelled by demodulating with higher (odd) harmonics[1,3]. The simplest waveform that achieves this consists of the fundamental and third harmonics:

$$D(t) = \sqrt{2}\ [\ \sin[2\pi f_m t + \varphi(t)] + \ \gamma\ \sin[6\pi f_m t + 3\varphi(t) + \theta]\ ] \quad (7)$$

where γ and θ are the relative amplitude and phase of the third harmonic with respect to the fundamental. Substituting Eqs. (7) and (4) into Eq. (3) gives the demodulated shot noise power spectrum:

$$P_n(f,t) = \ P_{sql}\ [\ 1 + {}^1/_2 \cos[2\varphi(t)] + \gamma^2 - \gamma\cos[2\varphi(t) + \theta]] \quad (8)$$

Again this spectrum is flat. The signal and non-signal quadratures are defined by $\varphi = 0$ and $\pi/2$ respectively. Setting $\gamma = 1/2$ and $\theta = 0$ reduces the in-phase noise to its minimum possible value, $1.25P_{sql}$, down from $1.5P_{sql}$ using the first harmonic only, a noise suppression of 0.8 dB[3].

Again, a time domain description illustrates the process. Consider the modulated noise shown in Fig. 1(a). Fig. 4 shows the resulting noise for various demodulating waveforms consisting of combinations of the first and third harmonics at different phases φ and θ. When $\theta = 0$, the phase dependence in the demodulated noise disappears. (Signal demodulation still requires $\varphi = 0$.) In contrast, when $\theta = \pi$, the resulting demodulating waveform is much more peaked, and more efficiently picks out the increased noise in the signal quadrature, greatly exaggerating the phase dependence.

The effect of rapidly scanning φ, while slowly varying θ is plotted from Eq. (8) in Fig. 5(a). This spectrum reflects the time domain predictions of Fig. 4. In particular, the demodulated noise limits are +3.5 dB and -6 dB for $\theta = \pi$ and +0.97 dB (constant) for $\theta = 0$.

Experimentally, a third harmonic is produced by doubling the fundamental and mixing it with the original (inside dashed box in Fig. 2). The residual fundamental is removed by a high-pass filter. The third harmonic is mixed with the non-stationary shot noise in a separate mixer (to prevent mixer saturation). The two mixer outputs are added at a signal combiner, and the output fed to a receiver. This operation is equivalent to combining the demodulation waveforms prior to mixing with the noise.

The demodulation phase $\varphi(t)$ is scanned by offsetting the demodulation frequency from 37.5 MHz. One mixer output is delayed by 0.48μs, enabling the waveform phase θ in Eq. (8) to be varied slowly by sweeping the receiver frequency, f ($\Delta\theta/\Delta f \sim 2\pi$ rad per 2.1 MHz). The third harmonic amplitude γ was set by a variable attenuator.

The experimental noise spectrum obtained with the combined harmonics is shown in Fig. 5(b) and measured spectra due to each harmonic alone are given in Fig 5(c) and 5(d). Good qualitative agreement is obtained with Fig. 5(a), in particular, strong undulations of the envelope as θ is varied, confirming that the two mixer outputs are correlated. Filter-induced spectral asymmetry is believed responsible for the incomplete nodes in the experimental spectrum in Fig. 5(b). This asymmetry also altered the optimum choice of γ. The use of optimised filters in future designs should

allow the expected noise reduction of 0.8 dB to be attained using the third harmonic.

In conclusion, we have demonstrated that fully sinusoidally modulated light produces non-stationary shot noise statistics. Simple demodulation led to a phase dependence of 4.8 dB peak-peak, including a 1.8 dB noise penalty in the signal quadrature, in close agreement with theory. We also observed that noise demodulated with the third harmonic was correlated with that due to the fundamental. In so doing, we have confirmed a simple time domain description of non-stationary shot noise demodulation, and demonstrated the feasibility of excess noise reduction in the signal quadrature by including higher harmonics in the demodulation waveform.

This project was supported by a grant from the Australian Research Council. M. Gray is a recipient of an Australian National University Graduate Scholarship.

References

1. B. J. Meers and K. A. Strain, Phys. Rev. A. 44, 4693 (1991).

2. A. J. Stevenson, M. B. Gray, H. A. Bachor and D. E. McClelland, submitted to Appl. Opt. (1992).

3. T. M. Niebauer, R. Schilling, K. Danzmann, A. Rudiger, and W. Winkler, Phys. Rev. A. 43, 5022 (1991).

4. N. Mio and K. Tsubono, Phys. Lett. A. 164, 255 (1992).

5. H. -A. Bachor and P. J. Manson, J. Mod. Opt. 37, 1727 (1990).

Figure Captions

Fig. 1 **(a)** Non-stationary noise $i_n(t)$ = white noise $\times \sin^2[2\pi f_m t]$. **(b)** $i(t) \times D(t)$; $(D(t) = \sin[2\pi f_m t].)$ **(c)** $i(t) \times D(t)$; $(d(t) = \cos[2\pi f_m t].)$

Fig. 2. Experimental arrangement for measuring phase dependence of non-stationary shot noise.

Fig. 3. **(a)** Demodulated noise power at 10 MHz (using fundamental harmonic only). RBW = 100 kHz, VBW = 100 Hz. **(b)** As in (a), but sweeping demodulation frequency offset through 0 Hz.

Fig. 4. D(t) and demodulated noise $i_n(t) \times D(t)$: **(a)** $\varphi = 0, \theta = 0$ **(b)** $\varphi = \pi/2, \theta = 0$ **(c)** $\varphi = 0, \theta = \pi$ **(d)** $\varphi = \pi/2, \theta = \pi$.

Fig. 5. **(a)** Theoretical demodulated noise, in dB relative to P_{sql}, $\gamma = 0.5$, $\varphi(t)$ scanned rapidly, θ varied slowly. **(b)** Experimental noise using 1st & 3rd harmonics, $\gamma = 0.36$. **(c)** Experimental noise using 1st harmonic (37.5 MHz) only. **(d)** Experimental noise using 3rd harmonic (112.5 MHz) only.

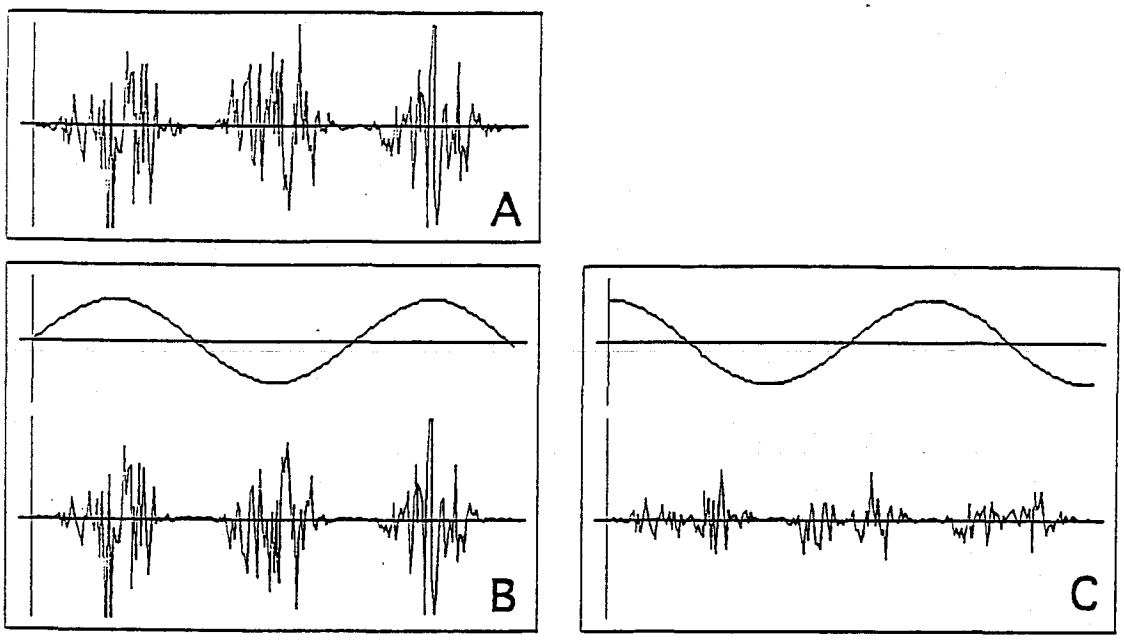

Figure 1

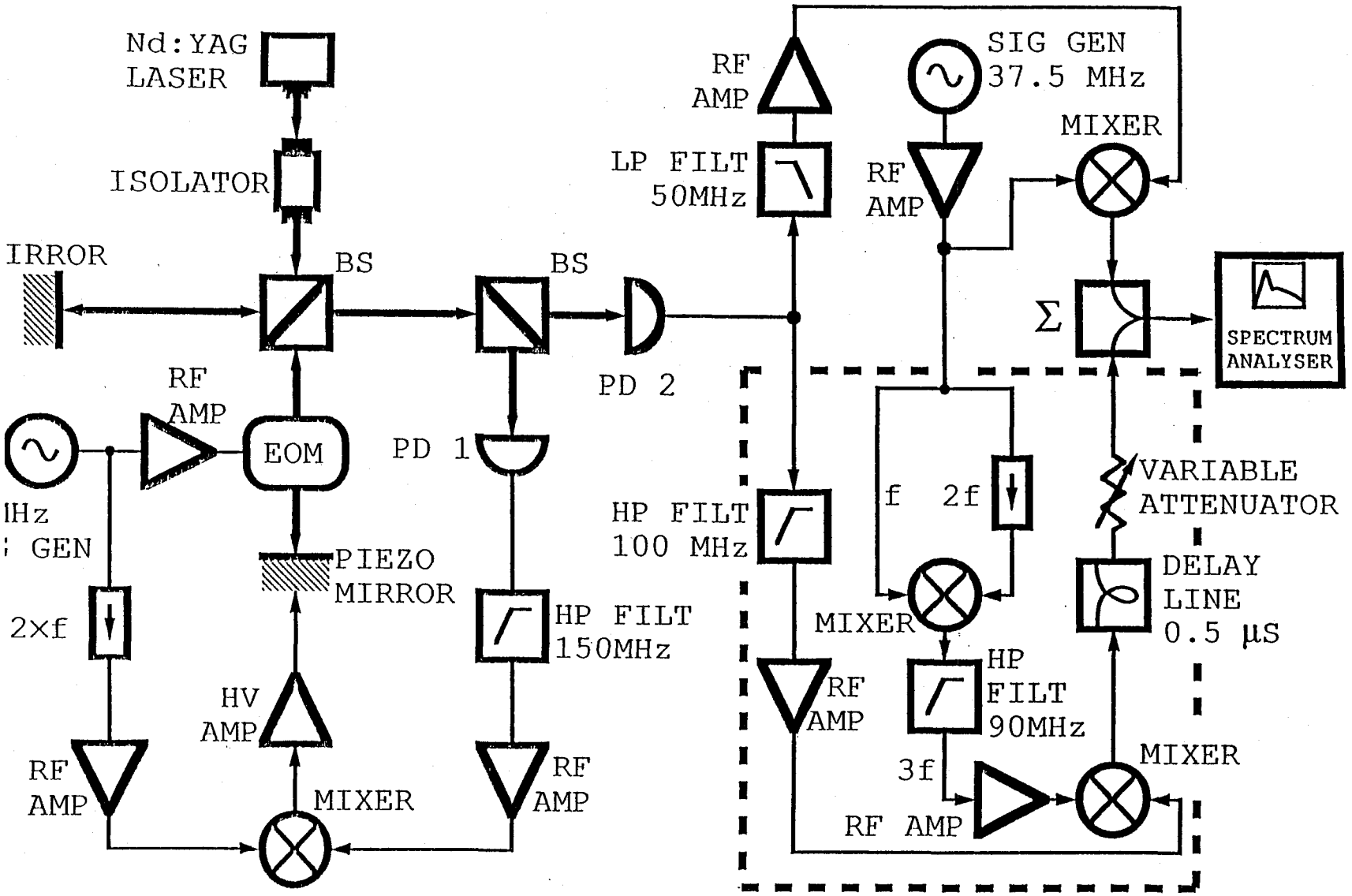
Nd:YAG
LASER
ISOLATOR
IRROR
BS
BS
RF
AMP
EOM
PD 1
PD 2
IHz
; GEN
2×f
PIEZO
MIRROR
HP FILT
150MHz
HV
AMP
RF
AMP
MIXER
RF
AMP
RF
AMP
LP FILT
50MHz
SIG GEN
37.5 MHz
RF
AMP
MIXER
Σ
SPECTRUM
ANALYSER
HP FILT
100 MHz
f
2f
VARIABLE
ATTENUATOR
DELAY
LINE
0.5 µS
MIXER
RF
AMP
HP
FILT
90MHz
3f
RF AMP
MIXER

Figure 2

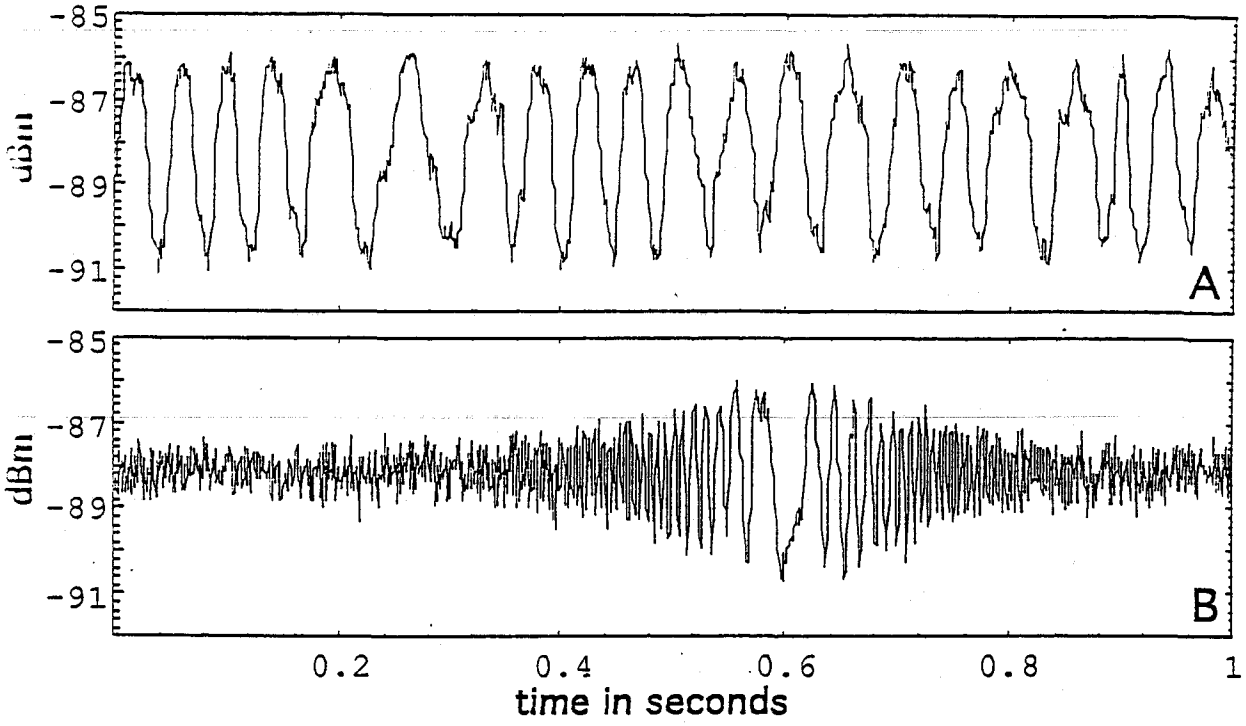

Figure 3

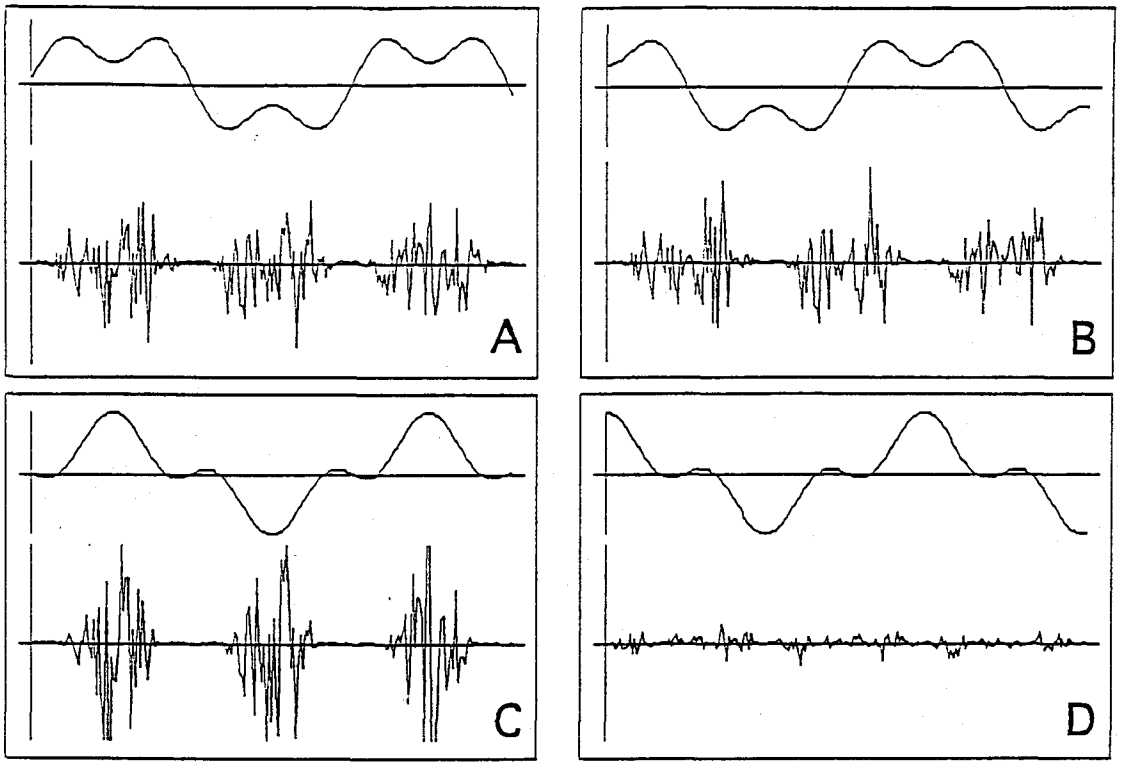

Figure 4

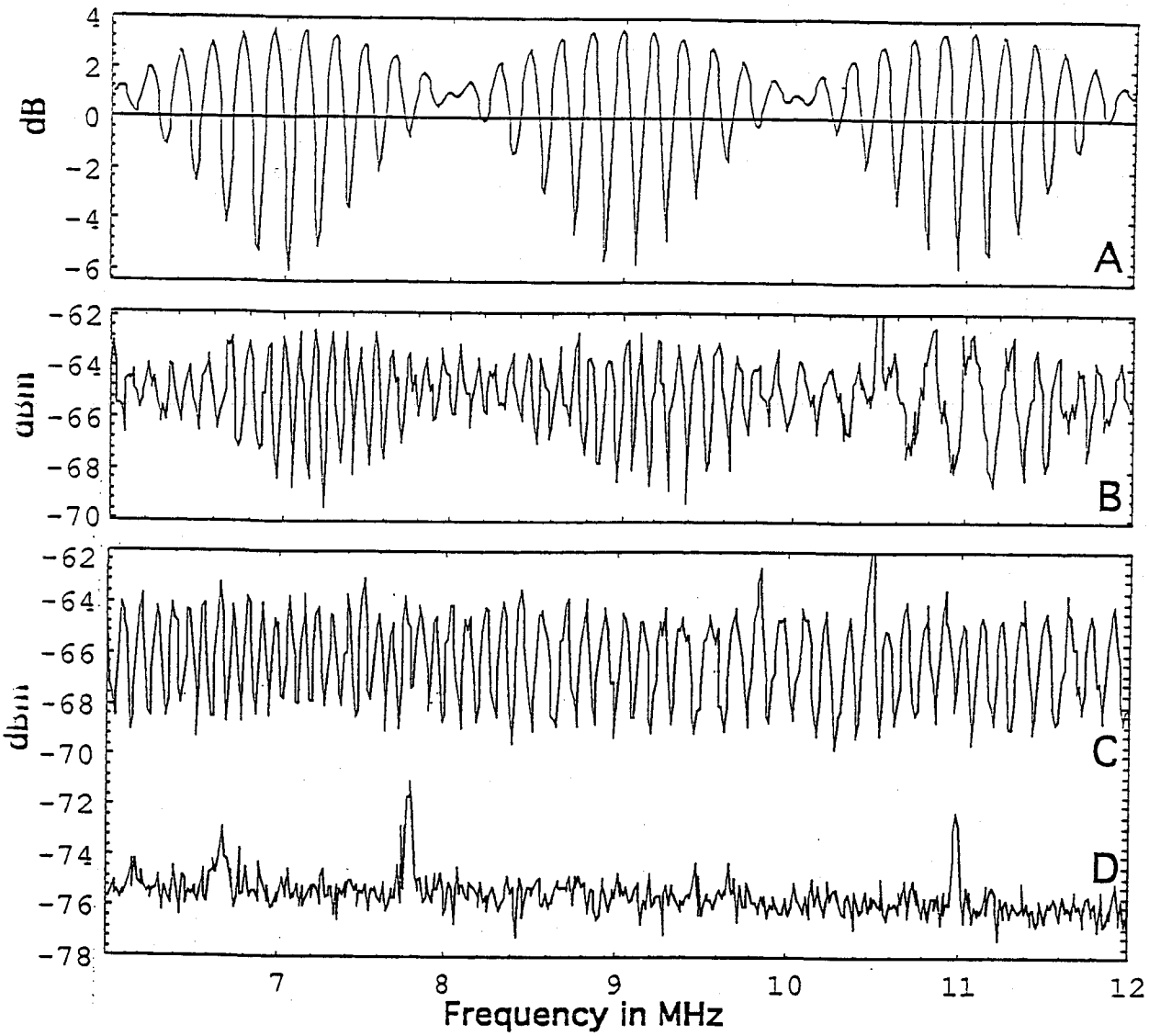
4
2
0
-2
-4
-6
dB
A
-62
-64
-66
-68
-70
dBm
B
-62
-64
-66
-68
-70
-72
-74
-76
-78
dBm
C
D
7
8
9
10
11
12
Frequency in MHz

Figure 5